

# ProBDNF and its receptors are upregulated in glioma and inhibit the growth of glioma cells in vitro

Jing Xiong\*, Li Zhou\*, Miao Yang, Yoon Lim, Yu-hong Zhu, Deng-li Fu, Zhi-wei Li, Jin-hua Zhong, Zhi-cheng Xiao, and Xin-Fu Zhou

*Key Laboratory of Stem Cells and Regenerative Medicine, Institute of Molecular and Clinical Medicine, Kunming Medical University, Kunming, Yunnan Province, PR China (J.X., L.Z., Z.-C.X., X.-F.Z.); School of Pharmacology and Medical Sciences, University of South Australia, Adelaide, Australia (M.Y., Y.L., J.-H.Z., X.-F.Z.); the Second Affiliated Hospital of Kunming Medical University, Kunming, Yunnan Province, PR China (J.X., Y.-H.Z., D.-L.F., Z.-W.L.); Department of Immunology and Stem Cell Laboratories, Monash University, Clayton, Victoria, Australia (Z.-C.X.)*

**Background.** High-grade glioma is incurable, with a short survival time and poor prognosis. The increased expression of p75 neurotrophin receptor (NTR) is a characteristic of high-grade glioma, but the potential significance of increased p75NTR in this tumor is not fully understood. Since p75NTR is the receptor for the precursor of brain-derived neurotrophic factor (proBDNF), it is suggested that proBDNF may have an impact on glioma.

**Methods.** In this study we investigated the expression of proBDNF and its receptors p75NTR and sortilin in 52 cases of human glioma and 13 cases of controls by immunohistochemistry, quantitative real-time PCR, and Western blot methods. Using C6 glioma cells as a model, we investigated the roles of proBDNF on C6 glioma cell differentiation, growth, apoptosis, and migration in vitro.

**Results.** We found that the expression levels of proBDNF, p75NTR, and sortilin were significantly increased in high-grade glioma and were positively correlated with the malignancy of the tumor. We also observed that tumors expressed proBDNF, p75NTR, and sortilin in the same cells with different subcellular distributions, suggesting an autocrine or paracrine loop. The ratio of proBDNF to mature BDNF was decreased in high-grade glioma tissues and was negatively correlated with tumor grade.

Using C6 glioma cells as a model, we found that proBDNF increased apoptosis and differentiation and decreased cell growth and migration in vitro via p75NTR.

**Conclusions.** Our data indicate that proBDNF and its receptors are upregulated in high-grade glioma and might play an inhibitory effect on glioma.

**Keywords:** brain-derived neurotrophic factor, glioma, human, proBDNF, p75NTR, sortilin.

Malignant glioma is the third leading cause of cancer-related deaths among 15- to 54-year-old men and women.<sup>1,2</sup> Despite optimized surgery, radiotherapy, and chemotherapy,<sup>3–7</sup> the median survival time of high-grade glioma is 9 months, and only 5%–10% of patients can survive up to 2 years.<sup>8</sup> The etiology of glioma is not fully understood. It is believed that human malignant glioma arises from neural progenitor cells and/or dedifferentiated astrocytes.<sup>9–15</sup> These tumors tend to occur in the cerebral hemispheres, typically at the cortical/subcortical interface.<sup>16</sup> Malignant glioma cells are extremely infiltrative, often migrating along the basement membrane of blood vessels or along myelinated white matter but rarely metastasizing outside the central nervous system.<sup>17</sup>

How malignant glioma cells infiltrate and quickly migrate away from tumor mass is not clear. Recent studies have shown that the neurotrophin receptor (NTR) p75NTR plays a central role in the quick migration and infiltration of glioma cells into normal brain tissues and is likely a therapeutic target.<sup>18</sup> However, the mechanism of p75NTR responsible for triggering and activating the migration of these cells is not known. Neurotrophins, including nerve growth factor (NGF), brain-derived

Received October 27, 2012; accepted February 20, 2013.

\*These authors contributed equally to this work.

**Corresponding Authors:** Xin-Fu Zhou, PhD, School of Pharmacology and Medical Sciences, University of South Australia, Adelaide 5000, Australia (xin-fu.zhou@unisa.edu.au); Zhi-cheng Xiao, PhD, Department of Immunology and Stem Cell Laboratories, Monash University, Clayton 3168, Victoria, Australia (zhicheng.xiao@monash.edu).

neurotrophic factor (BDNF), neurotrophin (NT)-3, and NT-4/5, bind to p75NTR and play important roles in brain function and development. BDNF is the most studied neurotrophin produced by astrocytes and neurons.<sup>19–21</sup> It is first synthesized as a precursor of BDNF (proBDNF) and is subsequently cleaved either intracellularly by prohormone convertases and/or furin or extracellularly by plasmin and matrix metalloproteases (MMPs) to release mature homodimeric proteins (mature BDNF).<sup>22,23</sup>

ProBDNF is present in many regions of the CNS<sup>24</sup> and is released in cultured cortical neurons and at hippocampal synapses.<sup>25,26</sup> ProBDNF binds to both p75NTR and the coreceptor sortilin with a high affinity,<sup>26</sup> which induces apoptosis,<sup>26–28</sup> long-term depression,<sup>29</sup> synaptic retraction,<sup>30–32</sup> and neurite collapse.<sup>33</sup> Because proBDNF induces cell apoptosis and has inhibitory effects on neuronal events, it may be important to characterize the expression profile of proBDNF and its receptors in human glioma, which might provide therapeutic targets for clinical intervention.

In the present study, we investigated, for the first time, the expression of proBDNF and its receptors p75NTR and sortilin in human glioma. We also examined the potential role of proBDNF in glioma using the C6 glioma cell line.

## Materials and Methods

### Patients

All patients ( $N = 65$ ) included in this study were enrolled from the Department of Neurosurgery and the Department of Oncology of the Second Affiliated Hospital of Kunming Medical University, Yunnan, China. The use of human material in this study was approved by the ethics committee of Kunming Medical University. Informed consent forms were signed by all patients, authorizing the use of their tissues in the present investigation. Of 65 cases, 52 underwent resection of glioma and none received radiotherapy or chemotherapy. All tumor specimens were classified and graded according to the 2007 World Health Organization (WHO) classification of tumors of the CNS<sup>34</sup> by 2 independent pathologists with full diagnostic agreement. Patient characteristics are shown in Supplementary Table S1. The 52 glioma samples included 9 cases of WHO grade I (all pilocytic astrocytomas), 23 cases of grade II (18 astrocytomas, 4 ependymomas, 1 oligodendroglioma), 15 cases of grade III (13 anaplastic astrocytomas, 1 anaplastic ependymoma, 1 anaplastic oligoastrocytoma), and 5 cases of grade IV (all glioblastomas). For the convenience of analysis, we divided all gliomas into 2 groups: the low-grade group included grades I and II ( $n = 32$ ; mean age:  $34.34 \pm 15.22$  y; 17 males and 15 females), and the high-grade group included grades III and IV ( $n = 20$ ; mean age:  $46 \pm 15.35$  y; 11 males and 9 females).

Tumors were localized in the frontal lobe ( $n = 28$ ), temporal lobe ( $n = 15$ ), parietal lobe ( $n = 9$ ), occipital lobe ( $n = 4$ ), and ventricles ( $n = 7$ ). There were 14 tumors involving multiple lobes.

Nonneoplastic brain tissues ( $n = 13$ ) were used as controls. These patients were subjected to lobe resection for epilepsy surgery ( $n = 3$ ; mean age:  $37.66 \pm 10.98$  y; 2 males and 1 female), brain trauma ( $n = 4$ ; mean age:  $36.75 \pm 11.14$  y; all males), and hypertensive cerebral hemorrhage ( $n = 2$ ; mean age:  $63.3 \pm 2.82$  y; all males) and underwent internal decompression. Normal tissues near the tumor ( $n = 4$ ; mean age:  $35 \pm 5.71$  y; 2 males and 2 females) were also included. Control tissues were acquired from the frontal lobe ( $n = 6$ ), temporal lobe ( $n = 4$ ), parietal lobe ( $n = 1$ ), and cerebellum ( $n = 2$ ).

### Tissue Preparation

During surgery, resected tissues from the tumors and controls were collected, snap-frozen in liquid nitrogen, and stored at  $-80^{\circ}\text{C}$  for Western blot analysis and quantitative real-time (qRT) PCR assay. Small fragments of tissue were washed in phosphate buffered saline (PBS), fixed in 10% formalin, and embedded in paraffin according to standard immunohistochemistry (IHC) procedure.

### C6 Cell Culture

C6 glioma cells were grown in low-glucose Dulbecco's modified Eagle's medium (DMEM; Gibco) supplemented with 10% fetal bovine serum (FBS; Gibco) or otherwise as specified, 1% glutamate, and 1% penicillin/streptomycin at  $37^{\circ}\text{C}$  in a humidified atmosphere of 5%  $\text{CO}_2$  and 95% air.

### Immunohistochemistry and Immunocytochemistry

Serial 5- $\mu\text{m}$ -thick sections of paraffin-embedded tissues were cut using a microtome, mounted on polylysine-coated slides, and processed for IHC. Briefly, single-label IHC was carried out using the avidin–biotin peroxidase method and diaminobenzidine as a chromogen. The sections were deparaffinated in xylene, rinsed in ethanol (100% to 75%) and incubated with 3%  $\text{H}_2\text{O}_2$  for 10 min. The section slides were subjected to antigen retrieval using a pressure cooker and then washed with PBS (pH 7.4). After being incubated with 10% normal horse serum for 1 h for blocking, the section slides were incubated with the primary antibodies (see Table 1) at  $4^{\circ}\text{C}$  overnight. After incubation with the primary antibodies, section slides were washed with PBS 3 times and incubated with the appropriate biotinylated secondary antibody (1:200 donkey anti-goat or 1:200 donkey anti-rabbit immunoglobulin; Santa Cruz) at room temperature for 1 h. All section slides were incubated with avidin–biotin peroxidase complex (Vectastain ABC kit, Vector Labs) at room temperature for 30 min, then were developed in a solution of diaminobenzidine and counterstained with hematoxylin. The section slides were dehydrated through a series of alcohol washes and coverslipped. In this experiment, primary antibody omission controls were used as negative controls. Sections were observed by using a light microscope (Leica). Positive immunostaining, which appeared as a yellow to brown color,

**Table 1.** Primary antibodies for IHC/ICC or Western blot assays

Primary Antibody	Source	Dilution for IHC/ICC	Dilution for Western Blot
Sheep anti-proBDNF	Provided by Prof Zhou Lab	1:500	1:500
Rabbit anti-proBDNF	Provided by Prof Zhou Lab	1:400	
Sheep anti-mature BDNF	Provided by Prof Zhou Lab		1:200
Rabbit anti-sortilin	Abcam	1:1000	1:1000
Goat anti-p75NTR	Santa Cruz	1:200	1:200
Rabbit anti-SP1	Abcam		1:500
Mouse anti- $\beta$ -actin	Sigma		1:1000
Mouse anti- $\beta$ -tubulin	Sigma		1:1000
Rabbit anti-GFAP	Abcam	1:500	1:1000

and its intensity were clearly higher than the background staining. Five to 10 representative fields at 400 $\times$  magnification per slide were observed. The intensity of the positive reaction was scored as 0 = negative (same as the background), 1 = light staining, 2 = moderate staining, and 3 = intense staining. Additionally, the number of positive cells was classified as (i) negative (-, no positive cells found), (ii) weakly positive (+,  $\leq 25\%$  cells positive), (iii) moderately positive (++, 26%–50% cells positive), and (iv) intensely positive (+++, over 50% cells positive), as described.<sup>35</sup> IHC staining was assessed semiquantitatively by measuring both the intensity of the staining and the number of positive cells. The scores for the intensity and the percentage of positive cells were multiplied to give a weighted score for each case. The mean weighted scores in 3 groups were compared for statistical analysis.<sup>36</sup>

For C6 cell staining, cells were cultured on coverslips and fixed with 4% paraformaldehyde in PBS at room temperature for 20 min. Immunocytochemistry (ICC) for proBDNF, p75NTR, and sortilin was performed as for IHC.

#### Fluorescence Double Labeling of Tumors and Controls

Before primary antibody incubation, the section slides were permeabilized and blocked with PBS/0.5% Triton X-100/10% donkey serum at room temperature for 60 min. The sections were incubated in proBDNF/p75NTR and proBDNF/sortilin antibodies diluted in PBS/0.5% Triton X-100/5% donkey serum at 4°C overnight. The primary antibodies used for immunofluorescence are summarized in Table 1.

The sections were then washed 3 times with PBS/0.3% Triton X-100, each time for 15 min. The sections were incubated with the secondary antibodies donkey anti-rabbit Alexa 546 (red, 1:1000; Invitrogen) and donkey anti-goat

Alexa 488 (green, 1:1000; Invitrogen) in the dark for 1 h. The section slides were washed 3 times with PBS and mounted with media containing 4',6'-diamidino-2-phenylindole (DAPI; Vector Labs).

Coexpression of proBDNF/p75NTR and proBDNF/sortilin was assayed by immunofluorescence double-labeling. The section slides were observed and photographed using a Leica confocal microscope.

#### Protein Extraction

Tissues from human controls and glioma samples were homogenized in lysis buffer containing 50 mM Tris HCL, pH 7.4, 150 mM NaCl, 1% nonyl phenoxyethoxyethanol (NP)40, 1% sodium deoxycholate, 0.1% sodium dodecyl sulfate (SDS) and protease inhibitor cocktail (Roche), plasminogen activator inhibitor 1 (PAI-1; Sigma), and furin inhibitor 1 (Calbiochem), vortexed, and centrifuged for 20 min at 13 000 rpm at 4°C. The addition of PAI-1 and furin inhibitor 1 was to prevent the conversion of proBDNF to mature BDNF. The C6 cells were harvested with lysis buffer as in the previous procedure and centrifuged at 4°C at 13 000 rpm for 20 min. Nuclear protein extraction was performed using NE-PER Nuclear and Cytoplasmic Extraction Reagents (ThermoFisher) according to manufacturer's instructions. Protein content was determined using a bicinchoninic acid kit (CoWin Biotechnology). Protein was stored at -80°C until analysis.

#### Western Blots

For Western blot, 50  $\mu$ g/lane was subjected to SDS-polyacrylamide gel electrophoresis in 10% or 12% gels at 100 V for 2 h. Separated proteins were transferred onto polyvinylidene difluoride membranes in transfer buffer (48 mM Tris, 39 mM glycine, 0.037% weight/volume [w/v] SDS, 20% volume/volume [v/v] methanol) with 400 mA at 4°C for 1.5 h, using a wet electroblotting system (Bio-Rad). The membranes were then blocked in blocking buffer (20 mM Tris, pH 8.0, 150 mM NaCl, 0.05% [v/v] Tris-buffered saline and 0.05% Tween 20 [TBST], 5% [w/v] nonfat milk) for 2 h at room temperature and incubated overnight at 4°C with primary antibodies in TBST containing 5% nonfat milk (see Table 1 for the primary antibodies used in the present study). After several washes in TBST, the membranes were incubated with the appropriate horseradish peroxidase-conjugated secondary antibodies (goat anti-rabbit or anti-mouse, donkey anti-goat in TBST + 5% nonfat milk, 1:1000; all Santa Cruz) for 2 h at room temperature. After a washing with TBST, immunoreactive bands were detected using an enhanced chemiluminescence kit (CoWin Biotechnology). The same membrane was probed with mouse anti- $\beta$ -tubulin or anti- $\beta$ -actin as a loading control. Densitometric analyses were performed using the Quantity One software program. Protein expression was determined in relative units in reference to  $\beta$ -tubulin or  $\beta$ -actin. Nuclear proteins were extracted with NE-PER Nuclear and Cytoplasmic Extraction

Reagents (ThermoFisher) and blotted with antibodies to the nuclear protein marker SP1 (specificity protein 1; Abcam) and the cytoplasmic protein marker  $\beta$ -tubulin (Sigma) to monitor potential contaminations from different fractions.

#### Enzyme-linked Immunosorbent Assay for Mature BDNF

Tissue samples were homogenized, and levels of mature BDNF in the homogenate were determined by a highly specific, mature BDNF enzyme-linked immunosorbent assay (ELISA) kit developed in-house. Briefly, sterile immunoplates were coated with 100  $\mu$ L/well of protein G-purified monoclonal mouse antibodies to mature BDNF (2  $\mu$ g/mL in coating buffer [50 mM carbonate, pH 9.6]) for an overnight incubation. After being washed 3 times with 0.05% (v/v) Tween-20 in PBS (pH 7.4) after each step, the plates were blocked with 3% bovine serum albumin (150  $\mu$ L/well) and incubated for 1 h at 37°C. Subsequently, 100  $\mu$ L homogenate of tissue samples and different concentrations of standard mature BDNF were added in plates for 1 h incubation at 37°C. The plates were washed and incubated in 100  $\mu$ L/well of biotin-conjugated sheep anti-mature BDNF (2.5  $\mu$ g/mL in 0.1% bovine serum albumin, 0.05% [v/v] Tween-20 in Tris-buffered saline, pH 7.4) at 37°C for 1 h. After extensive washing, streptavidin-horseradish peroxidase was added in the plates. Color was developed in 3,3',5,5'-tetramethylbenzidine substrates and stopped in 1 M sulfuric acid (50  $\mu$ L/well). The plate was analyzed with an enzyme immunoassay (EIA) plate reader at a wavelength of 450 nm (Thermo).

Relative ratio of proBDNF and mature BDNF expression was determined by proBDNF in reference to  $\beta$ -tubulin in Western blot to mature BDNF in an ELISA assay.

#### Total RNA Extraction and cDNA Synthesis

Total RNA was extracted from tissues using Trizol reagent (Invitrogen) according to the manufacturer's instructions. RNA quantification/purification was determined by measuring A260:A280 ratios. A ratio close to 2.0 was considered a satisfactory level of homogeneity. Denaturing agarose gel electrophoresis was also used to assess the quality of the samples by observing 28S and 18S RNA bands. Then cDNA was synthesized from 1  $\mu$ g total RNA in a final reaction volume of 20  $\mu$ L. Briefly, a mixture of total RNA, oligo(deoxythymine), deoxyribonucleotide triphosphate mix, and diethylpyrocarbonate-treated distilled water was incubated for 5 min at 65°C. Then 5 $\times$  first chain solution and 0.1 M dithiothreitol were added, prior to incubation for 2 min at 37°C. Next, Moloney murine leukemia virus reverse transcriptase was added and incubated for 30 min at 37°C and followed incubation at 70°C for 15 min. The resulting cDNA was used for qRT-PCR.

#### Quantitative RT-PCR

The expression levels of the *BDNF* gene, the *NGFR* (p75NTR) gene, and the *SORT1* (sortilin) gene in both control brain tissues and gliomas of different malignancy grades were determined by qRT-PCR. Quantitative data were normalized relative to the internal housekeeping genes, such as *ACTB* ( $\beta$ -actin). Primer sequences were as follows (5'-3'): *BDNF* forward: TACTTTGGTTGCATGAAGGCTGCC, reverse: ACTTGACTACTGAGCATCACCCTG; *NGFR* forward: GTGGGACAGAGTCTGGGTGT, reverse: AAGGAGGGGAGGTGATAGGA; *SORT1* forward: TTGATGATCTCAGAGGCTCAG, reverse: TGAAGATTCTTCTCCACGAC; *ACTB* forward: CGGGAAATCGTGCGTGAC, reverse: TGGAAGGTGGACAGCGAGG; synthesized by Invitrogen. Each SYBR Green reaction (total volume, 20  $\mu$ L) contained 1 $\times$  FastStart Universal SYBR Green master (Roche Diagnostic), 0.5  $\mu$ M forward and reverse primers, and 0.5  $\mu$ g cDNA. Reactions were run on an ABI 7300 Real-Time PCR System (Applied Biosystems). The cycle conditions were initial denaturation at 95°C for 10 min, and 40 cycles of 15 s each at 95°C, and 60°C for 1 min. A DNA melting curve analysis was performed. The results of the qRT-PCR analysis were normalized to *ACTB*. Samples were confirmed to be free of DNA contamination by performing reactions without reverse transcriptase. All reactions were performed twice on each preparation. Data were analyzed using the  $2^{-\Delta\Delta C_t}$  method.<sup>37,38</sup>

#### Cell Viability Assay

To investigate the effect of endogenous and exogenous proBDNF on C6 cell growth and viability, we performed an MTT assay (3-(4, 5-dimethylthiazol-2-yl)-2, 5-diphenyltetrazolium bromide; Sigma). Cells were plated in 96-well plates at a density of 15 000 per well and treated at 60%–70% confluence. On the day of the experiment, the cells were rinsed twice with serum-free medium and treated with recombinant proBDNF protein (1, 3, 10, 30 ng/mL), anti-proBDNF (1, 3, 10  $\mu$ g/mL), or 5  $\mu$ g/mL p75NTR-ECD-Fc (an extracellular domain of p75NTR fused with an Fc fragment of immunoglobulin G) dissolved in serum-free media and media containing 5% FBS. Each treatment was performed in triplicate. Control remained untreated. The treated cells were incubated for 24–48 h at 37°C in 5% CO<sub>2</sub>. MTT assays were performed at 0, 24, and 48 h. The MTT reagent was reconstituted in PBS to 5 mg/mL. MTT-labeling reagent (20  $\mu$ L) was added to each well, the plates were incubated at 37°C for 4 h, and dimethyl sulfoxide solubilization solution (150  $\mu$ L) was added to each well. The absorbance of the samples was measured at 560 nm (EIA reader; Thermo) and correlated with living cell numbers. To minimize the variation among different assays, the data were corrected against control and plotted by using the optical density of control wells as 100% survival. The experiments were performed in duplicate and repeated at least 3 times.

### Cell Apoptosis Assay

To investigate the effect of endogenous and exogenous proBDNF on C6 cell apoptosis, apoptotic C6 cells were measured by DAPI stain as reported.<sup>39</sup> C6 cells were plated 15 000 per well in 96-well plates and cultured to 60%–70% confluence. On the day of the experiment, the cells were treated and prepared in serum-free medium as we have previously described here. After 48 h, C6 cells were fixed using 4% paraformaldehyde for 20 min and then stained with DAPI to visualize nuclei. Cell images were collected ( $\geq 5$  fields/well) using a Leica fluorescence microscope for each sample. The apoptotic and total number of nuclei were counted and their ratio calculated. To minimize the variation among different assays, we corrected against control.

### Scratch Assay

C6 cells ( $1.8 \times 10^5$ ) were plated in a 12-well plate and grown overnight to reach 95% confluence in 10% FBS-containing media. The monolayer cells were washed 3 times with serum-free DMEM and scratched with a 10- $\mu$ L pipette tip, washed with serum-free DMEM to remove floating cells, and photographed (0 h) at 100 $\times$  magnification. Monolayer cells with cell scratches were treated with recombinant proBDNF protein (1, 3, 10, 30 ng/mL), proBDNF antibody (1, 3, 10  $\mu$ g/mL), or p75NTR-ECD-Fc (5  $\mu$ g/mL). The cells were cultured in the serum-free medium for another 24 h and then photographed at the same position. The width of the cell scratch was measured using Adobe Photoshop 9.0 software. The relative migration distance was calculated by the formula:  $(A - B)/A$ , where  $A$  represents the mean width of the cell scratch before treatments and  $B$  represents the mean width of the cell scratch after treatments. Results were expressed as means  $\pm$  SE.

### Cell Invasion Assay

C6 cell invasion was examined using 24-well Boyden chemotaxis (Becton Dickinson). The upper culture chamber consisted of a polycarbonate filter with 8  $\mu$ m pore size coated with a uniform layer of Matrigel basement membrane matrix in the upper compartment of the chemotaxis chamber;  $3 \times 10^5$  cells per well were seeded into the upper compartment individually and incubated in 100  $\mu$ L serum-free media containing recombinant proBDNF (1, 3, 10, 30 ng/mL), antibodies to proBDNF (1, 3, 10  $\mu$ g/mL), or p75NTR-ECD-Fc (5  $\mu$ g/mL), while 750  $\mu$ L/well of media containing 20% FBS was placed in the bottom wells. Controls remained untreated. After 24 h incubation at 37°C in a CO<sub>2</sub> incubator, the cells on the upper surface of the inserts were gently wiped with a cotton swab. The cells on the lower surface of the inserts were fixed for 30 min with 4% paraformaldehyde, stained with DAPI. The cells in at least 5–10 random selected fields were photographed under a fluorescence microscope and counted. The data are presented as means  $\pm$  SE. In additional experiments, the cells on the

bottom of the insert were stained with cresyl violet solution (0.2%) for 15 min to confirm the DAPI stain data. After PBS washing, the dye was extracted with 10% acetic acid. Absorbance was measured at 570 nm using an EIA microplate reader (Thermo). The dye levels are directly proportional to the number of cells.<sup>40</sup>

### Statistical Analysis

The Kruskal–Wallis test, Mann–Whitney test, and Spearman rank correlation were applied to compare the differences between the control brain samples and glioma samples. The data of cell experiments from different groups were analyzed by 1-way ANOVA followed by post-hoc analysis of multiple comparisons. Differences were considered significant at  $P < .05$ .

## Results

### Expression of ProBDNF in Human Glioma Tissues

To investigate the expression of proBDNF and its receptors, p75NTR and sortilin, in the normal brain tissues and different grades of gliomas, we performed IHC, Western blot, and qRT-PCR assays. The proBDNF antibody used in this study was well characterized in our previous studies<sup>28,33,40</sup> and recognizes only proBDNF but not mature BDNF. ProBDNF-positive cells were detected in all normal brain and glioma tissues (Fig. 1A–C). ProBDNF was predominantly seen in the cytoplasm of neurons in normal tissues (Fig. 1A). There was a weak staining in the cytoplasm of tumor cells of low-grade gliomas (Fig. 1B). In contrast, strong proBDNF staining was shown in the cytoplasm and nuclei of high-grade gliomas (Fig. 1C). The intensity of immunostaining and the number of positive cells for proBDNF in high-grade gliomas were increased compared with low-grade gliomas and controls. The intensity of proBDNF staining appeared to be correlated with malignant progression. The distribution of proBDNF intensity among low-grade and high-grade tumors and control brain tissues is shown in Fig. 1D. All high-grade gliomas (100%) showed moderate to intense (++ to +++) proBDNF staining compared with low-grade gliomas (63.16%) and controls (46.15%). Semiquantitative analysis of proBDNF immunostaining showed that the difference in proBDNF score reached statistical significance in high-grade gliomas ( $P = .003$ ; Fig. 1E). This result was supported by Western blot data, which showed a significant increase of proBDNF expression in high-grade gliomas compared with low-grade gliomas and controls ( $P < .001$  Fig. 1G and H). The major proBDNF-like immunoreactive band corresponds to 34 kD. Two lower-molecular-weight bands at 23 and 17 kD were also observed and were most abundant in high-grade gliomas. After being normalized to  $\beta$ -tubulin, proBDNF showed a 1.40-fold increase from normal to low-grade (Fig. 1H) and a 3.32-fold increase from low-grade to high-grade ( $P = .001$ ; Fig. 1H). Quantitative RT-PCR also showed increased *BDNF* mRNA levels in high-grade gliomas

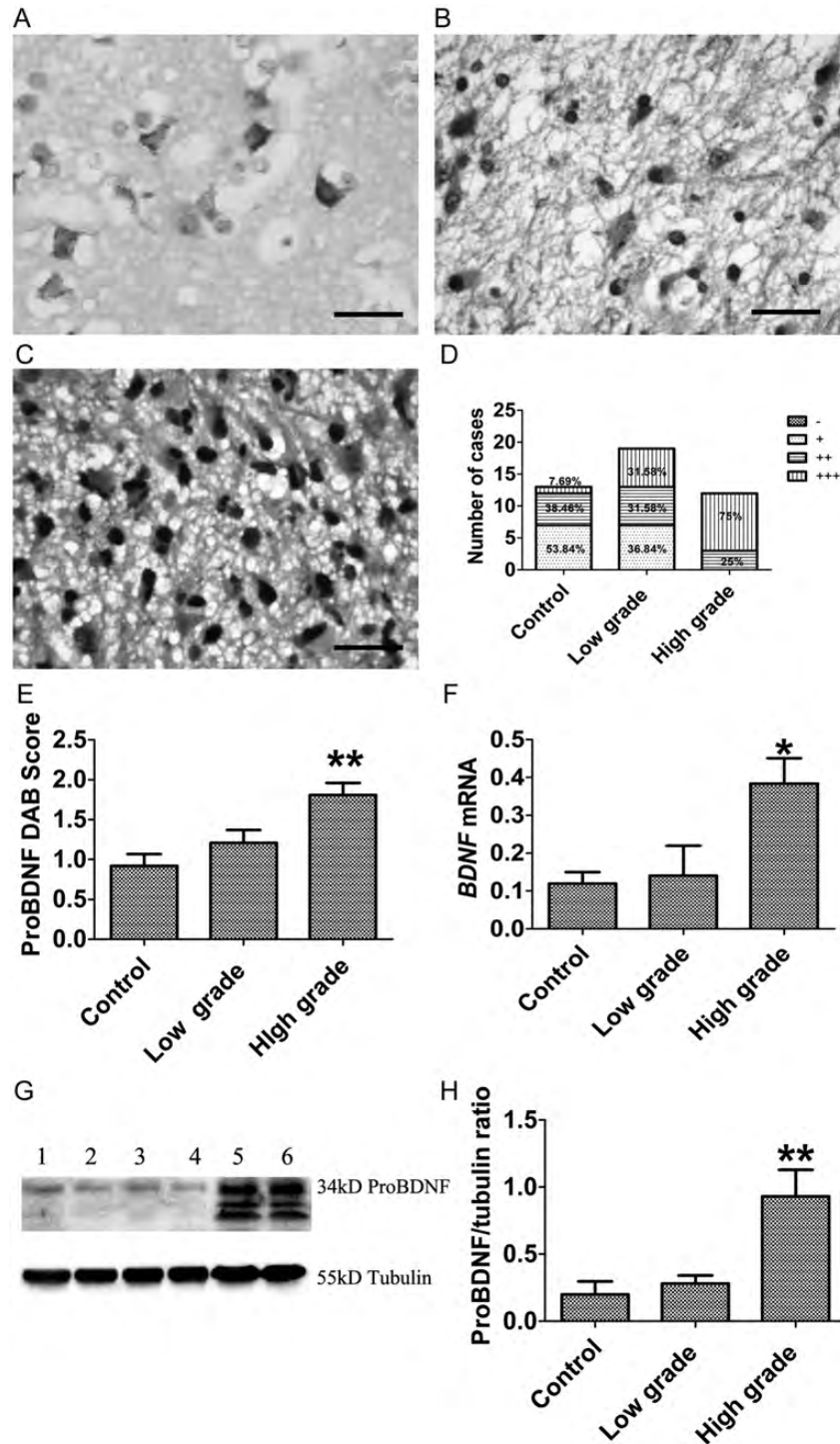


Fig. 1. Expression of proBDNF in human gliomas at different grades of malignancy. (A–E) IHC of proBDNF in glioma. ProBDNF staining is shown in (A) the neuronal cytoplasm of controls and (B) the cytoplasm of low-grade glioma cells. (C) High-grade glioma show an increase of proBDNF cytoplasmic and nuclear staining in tumor cells. (D) The percentage of proBDNF staining (–, +, ++, +++) in controls and low-grade and high-grade gliomas. (E) IHC of proBDNF staining was assessed semiquantitatively. ProBDNF intensity and percentage of positive cells were multiplied to give a weighted score for each case. Data were plotted as means  $\pm$  SE from control ( $0.92 \pm 0.15$ ,  $n = 13$ ) and low-grade ( $1.21 \pm 0.16$ ,  $n = 19$ ) and high-grade tumors ( $1.81 \pm 0.15$ ,  $n = 12$ ). ProBDNF staining was significantly increased in high-grade glioma (Kruskal–Wallis test,  $P = .003$ ). DAB, diaminobenzidine. (F) Examination of *BDNF* mRNA by qRT-PCR; data were normalized by *ACTB* and plotted as means  $\pm$  SE from controls ( $n = 9$ ) and low-grade ( $n = 16$ ) and high-grade tumors ( $n = 14$ ) (Kruskal–Wallis test,  $P = .014$ ). (G and H) Western blot of proBDNF using sheep anti-proBDNF antibody. (G) Duplicate samples were used for Western blot (lanes 1, 2: control; lanes 3, 4: low grade; lanes 5, 6: high grade). (H) A histogram was plotted as means  $\pm$  SE from controls ( $n = 10$ ), low-grade tumors ( $n = 21$ ), and high-grade tumors ( $n = 15$ ) (Kruskal–Wallis test,  $P < .001$ ) after being normalized by  $\beta$ -tubulin. Scale bar, 25  $\mu$ m. \* $P < .05$ . \*\* $P < .01$ .

( $P = .014$ ; Fig. 1F), which is consistent with the immunostaining and Western blot results.

#### *Expression of P75NTR in Human Glioma Tissues*

P75NTR staining was weakly present in the cytoplasm of neurons (Fig. 2A) in control and low-grade glioma cells (Fig. 2B). In contrast, high-grade tumors showed 71.45% of p75NTR staining (++ to +++), compared with controls (0%) and low-grade tumors (5.56%) (Fig. 2D). Semiquantitative analysis showed that p75NTR immunoreactivity in high-grade gliomas was significantly higher than in low-grade and control tissues ( $P < .001$ ; Fig. 2C and E). The increase of p75NTR expression in high-grade gliomas was supported by Western blot (Fig. 2G and H), showing a significant increase of p75NTR expression in high-grade gliomas ( $P < .001$ ). There was no significant difference in p75NTR level between low-grade gliomas and controls. Quantitative RT-PCR showed increased *NGFR* mRNA levels in high-grade gliomas ( $P = .032$ ; Fig. 2F), consistent with the results of immunostaining and Western blot results. Notably, expression profiles of both p75NTR and proBDNF were similar, showing increased expression parallel to the increase in tumor grade.

#### *Expression of Sortilin in Human Glioma Tissues*

Sortilin was stained from weak to moderate intensity in cytoplasm or membrane in neurons and glial cells of the control tissues and low-grade gliomas (Fig. 3A and B). High-grade gliomas showed a 50% moderate to intense (++ to +++) cytoplasmic staining (Fig. 3C and D). The expression pattern of sortilin was similar to that of proBDNF and p75NTR. Western blot showed a 95-kD immunoreactive band representing sortilin expression in human samples (Fig. 3G). Both *SORT1* mRNA analysis ( $P = .021$ ; Fig. 3F) and Western blot ( $P = .008$ ; Fig. 3G and H) showed increased sortilin in high-grade gliomas compared with controls and low-grade gliomas.

#### *Distribution of ProBDNF and P75NTR/Sortilin Receptors in Human Gliomas*

Confocal imaging showed that p75NTR was mainly in the cytoplasm of tumor cells, whereas proBDNF was present in both cytoplasm and nuclei (Supplementary Fig. S1A–H). The presence of proBDNF in nuclei was more obvious in high-grade tumors (Supplementary Fig. S1E–H). ProBDNF and sortilin were also colocalized in control tissues and glioma (Supplementary Fig. S2A–H) and both were increased in high-grade glioma (Supplementary Fig. S2E–H). To confirm the presence of proBDNF in nuclei, we extracted nuclear protein using a commercial reagent and probed with relevant markers. Indeed, we found a significant proportion of proBDNF in the nuclear fraction (Supplementary Fig. S3). Weaker sortilin expression was also detected in the nuclear fraction (Supplementary Fig. S3).

#### *Correlation Between Expression Levels of ProBDNF, P75NTR, and Sortilin and Malignancy Grades of Glioma*

Correlation analysis showed that proBDNF, p75NTR, and sortilin were positively related to the malignancy grade of glioma. Despite the popular correlation with glioma malignancy grade, the correlation coefficient between p75NTR and grade was largest (Spearman correlation analysis, proBDNF/grade:  $r = 0.567$ ,  $P = .001$ ; p75NTR/grade:  $r = 0.739$ ,  $P < .001$ ; sortilin/grade:  $r = 0.390$ ,  $P = .014$ ; Fig. 4A–C). Spearman correlation analysis also revealed certain interrelations between proBDNF and its receptors. There was a positive correlation between proBDNF and p75NTR levels ( $r = 0.621$ ,  $P < .001$ ; Fig. 4D), but no correlation was found between proBDNF and sortilin ( $r = -0.159$ ,  $P = .341$ ; Fig. 4E).

#### *Decreased Ratio of ProBDNF to Mature BDNF in Human High-grade Glioma*

To better understand the biological role of the increase in proBDNF found in high-grade gliomas, we also determined the ratio of proBDNF to mature BDNF in samples of different grades of glioma and control samples. Levels of mature BDNF were assayed by ELISA. The concentration of mature BDNF was significantly increased 1.97-fold from normal to low-grade ( $P < .001$ ; Fig. 5A) and 4.06-fold from low-grade to high-grade ( $P < .001$ ; Fig. 5A).

There was a positive correlation between proBDNF and mature BDNF levels (Spearman rank correlation,  $r = 0.822$ ,  $P < .001$ ; Fig. 5B). Though there was significant increase in proBDNF and mature BDNF levels in high-grade gliomas, mature BDNF exhibited a much greater increase. The ratio of proBDNF to mature BDNF exhibited a significant decrease of 17% in low-grade gliomas ( $P = .002$ ; Fig. 5C) and 44% in high-grade gliomas compared with control ( $P < .001$ ; Fig. 5C). The ratios of proBDNF to mature BDNF were negatively correlated with tumor grade (Spearman correlation,  $r = -0.35$ ,  $P = .02$ ; Fig. 5D).

#### *Expression of ProBDNF and Its Receptors (P75NTR and Sortilin) in C6 Cells*

To examine the effect of proBDNF, the C6 cell line was used in the present study. Immunostaining and Western blots showed the expression of proBDNF and its main receptors, p75NTR and sortilin, in C6 cells (Supplementary Fig. S4A–F). Western blots showed proBDNF also in the cell culture medium at the basal condition (Supplementary Fig. S4D). These results indicate that proBDNF may activate its receptors by an autocrine or paracrine mechanism in the behavior of C6 glioma cells.

#### *Effect of ProBDNF on Morphology and Differentiation of C6 Glioma Cells*

Treatment of C6 glioma cells with 30 ng/mL recombinant proBDNF for 24 h revealed a major morphological

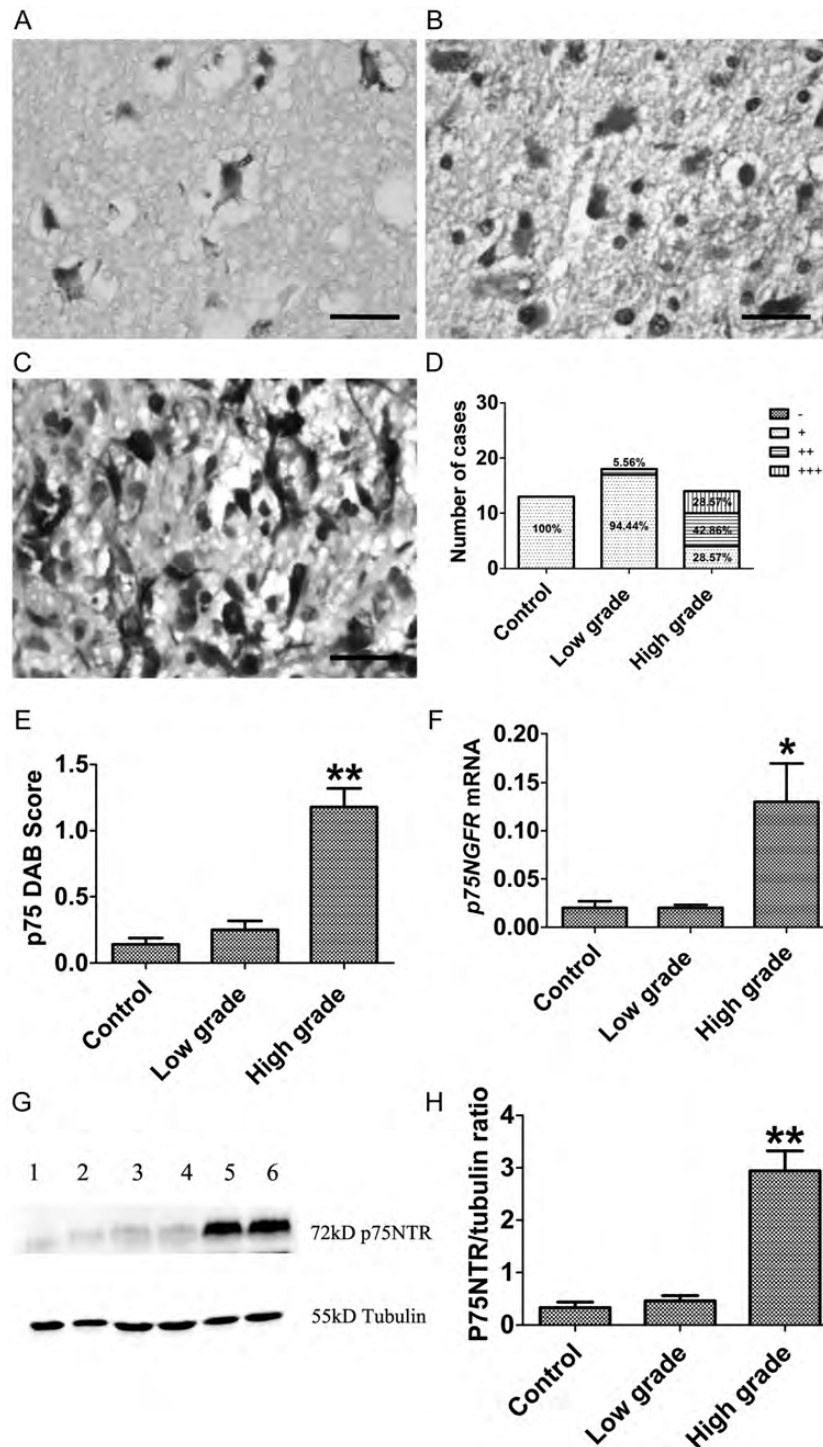


Fig. 2. Expression of p75NTR in human gliomas at different grades of malignancy. (A–E) IHC of p75NTR in glioma. (A) Controls showed weak p75NTR staining in the neuronal cytoplasm. (B) Low-grade glioma and (C) high-grade glioma show an increase of p75NTR staining in cytoplasm and nuclei. (D) Percentage of p75NTR staining (–, +, ++, +++) in controls and low-grade and high-grade gliomas. (E) IHC of p75NTR staining was assessed semiquantitatively. P75NTR intensity and percentage of positive cells were multiplied to give a weighted score for each case. Data were plotted as means  $\pm$  SE from control ( $0.14 \pm 0.05$ ,  $n = 13$ ) and low-grade ( $0.25 \pm 0.17$ ,  $n = 16$ ) and high-grade tumors ( $1.18 \pm 0.14$ ,  $n = 14$ ). A histogram shows that p75NTR staining is significantly increased in high-grade glioma (Kruskal–Wallis test,  $P < .001$ ). DAB, diaminobenzidine. (F) Examination of *NGFR* mRNA by qRT-PCR; data were normalized by *ACTB* and plotted as means  $\pm$  SE from controls ( $n = 7$ ), low-grade tumors ( $n = 14$ ), and high-grade tumors ( $n = 14$ ) (Kruskal–Wallis test,  $P = .032$ ). (G) Western blot of p75NTR using p75NTR polyclonal antibody; duplicate sample was used for Western blot (lanes 1, 2: control; lanes 3, 4: low grade; lanes 5, 6: high grade). (H) Histogram plotted as means  $\pm$  SE from controls ( $n = 10$ ), low-grade tumors ( $n = 17$ ), and high-grade tumors ( $n = 20$ ) (Kruskal–Wallis test,  $P < .001$ ). Scale bar, 25  $\mu$ m. \* $P < .05$ . \*\* $P < .01$ .



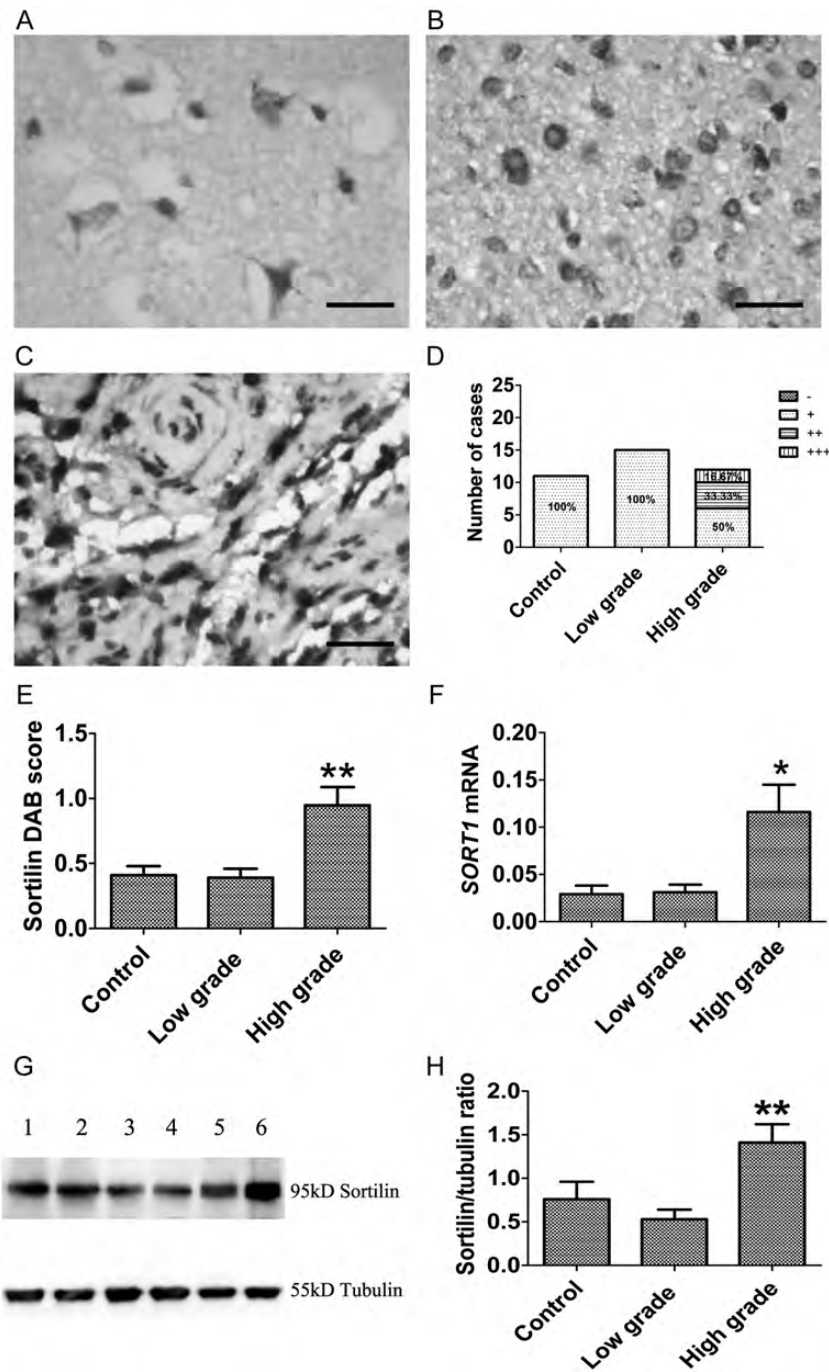


Fig. 3. Expression of sortilin in human glioma at different grades of malignancy. (A–E) IHC of sortilin in glioma. (A) Controls show weak sortilin staining in the neuronal cytoplasm and membrane. (B) Low-grade glioma and (C) high-grade glioma show an increase of sortilin staining in cytoplasm and nuclei. (D) The percentage of sortilin staining (–, +, ++, +++) in controls and low-grade and high-grade gliomas is shown. (E) IHC of sortilin staining was assessed semiquantitatively. Sortilin intensity and percentage of positive cells were multiplied to give a weighted score for each case. Data were plotted as means ± SE from controls ( $0.41 \pm 0.07$ ,  $n = 11$ ), low-grade tumors ( $0.39 \pm 0.07$ ,  $n = 15$ ), and high-grade tumors ( $0.95 \pm 0.14$ ,  $n = 12$ ). Sortilin staining was significantly increased in high-grade glioma (Kruskal–Wallis test,  $P < .001$ ). DAB, diaminobenzidine. (F) Examination of sortilin expression by qRT-PCR; data were normalized by *ACTB* and plotted as means ± SE from controls ( $n = 9$ ), low-grade tumors ( $n = 15$ ), and high-grade tumors ( $n = 15$ ) (Kruskal–Wallis test,  $P = .021$ ). (G and H) Western blot of sortilin using sortilin polyclonal antibody. (G) Duplicate samples were used for Western blot (lanes 1, 2: control; lanes 3, 4: low grade; lanes 5, 6: high grade). (H) A histogram was plotted as means ± SE from controls ( $n = 9$ ), low-grade tumors ( $n = 15$ ), and high-grade tumors ( $n = 15$ ) (Kruskal–Wallis test,  $P = .008$ ). Scale bar, 25  $\mu\text{m}$ . \* $P < .05$ . \*\* $P < .01$ .

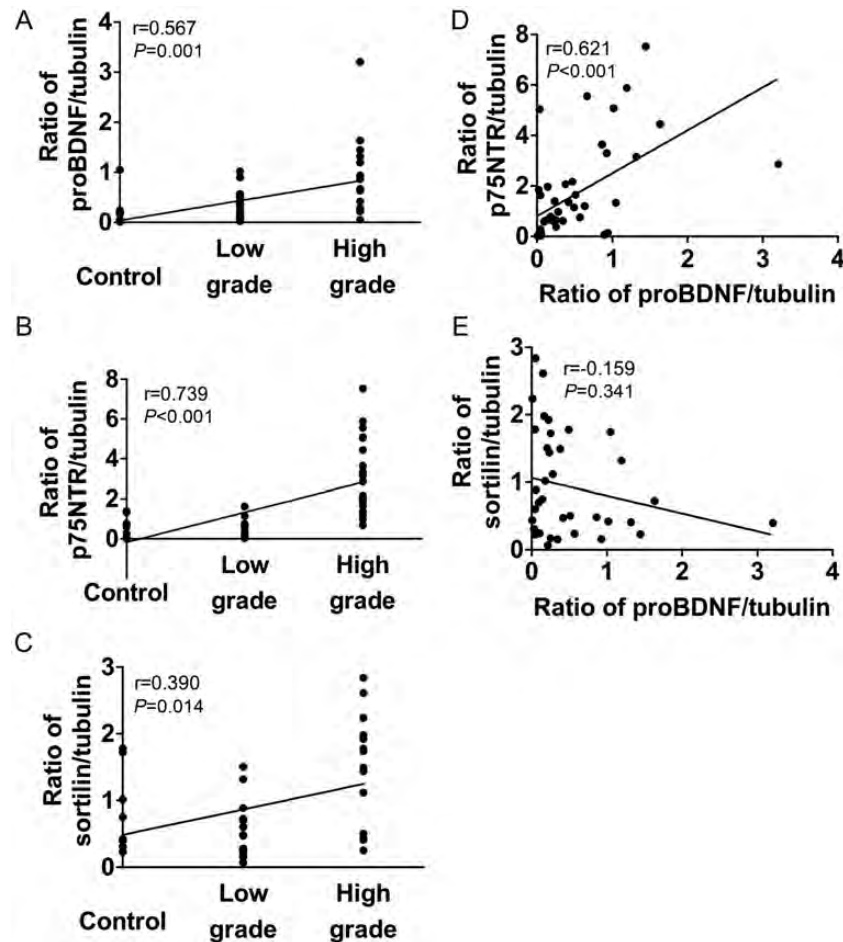


Fig. 4. Correlations of proBDNF and its receptors with tumor grade. (A) Ratio of proBDNF/tubulin vs grade. (B) Ratio of p75NTR/tubulin vs grade. (C) Ratio of sortilin/tubulin vs grade. (D) Ratio of proBDNF/tubulin vs ratio of p75NTR/tubulin. (E) Ratio of proBDNF/tubulin vs ratio of sortilin/tubulin.

transformation. The control cells displayed a flat polygonal appearance, whereas the treated cells showed a mature form characterized by a spindle shape with much longer, fine, tapering processes (Fig. 6A and B).<sup>41</sup> The cell morphological change was accompanied by cell differentiation. We further examined cell differentiation in the presence or absence of proBDNF by immunostaining and Western blot of glial fibrillary acidic protein (GFAP), a marker for mature astrocytes.<sup>42,43</sup>

GFAP staining in C6 cells was significantly decreased in the presence of anti-proBDNF (10  $\mu\text{g}/\text{mL}$ ) (Fig. 6C, D, and F), while staining was significantly increased after proBDNF treatment (30 ng/mL) (Fig. 6C, E, and F). Similarly, Western blots showed a significant decrease of GFAP protein in C6 cells treated with anti-proBDNF (3–10  $\mu\text{g}/\text{mL}$ ), while proBDNF induced an increase of GFAP at 48 h culture (Fig. 6G and H). To determine whether proBDNF induced differentiation of C6 cells through p75NTR, we used p75NTR-ECD-Fc to block proBDNF binding to p75NTR in the presence of proBDNF in the cell culture. C6 glioma cells were pre-treated with p75NTR-ECD-Fc (5  $\mu\text{g}/\text{mL}$ ) for 1 h, followed by treatment with proBDNF (30 ng/mL) for

48 h. Our results showed that p75NTR-ECD-Fc blocked the effect of proBDNF on increasing GFAP expression (Fig. 6G and H).

#### *ProBDNF Inhibited C6 Cell Growth Through P75NTR*

Upregulation of proBDNF in both C6 cells and high-grade gliomas suggests that proBDNF may play a role in glioma. To test this hypothesis, we first investigated the growth of C6 glioma cells by MTT and migration assays in the presence and absence of proBDNF or in the presence of p75NTR-ECD-Fc. MTT assays were performed in the presence of anti-proBDNF (1, 3, 10  $\mu\text{g}/\text{mL}$ ) to deplete endogenous proBDNF from either FBS-free or 5% FBS-containing cultures. Controls remained untreated. MTT assay showed that exogenous proBDNF significantly inhibited the growth of C6 cells in a dose-dependent manner, even at a concentration of 1 ng/mL in the absence of serum (Fig. 7A and C). However, the treatment of anti-proBDNF significantly promoted cell growth in a dose-dependent manner in the absence of serum (Fig. 7B and C). The inhibitory effect of

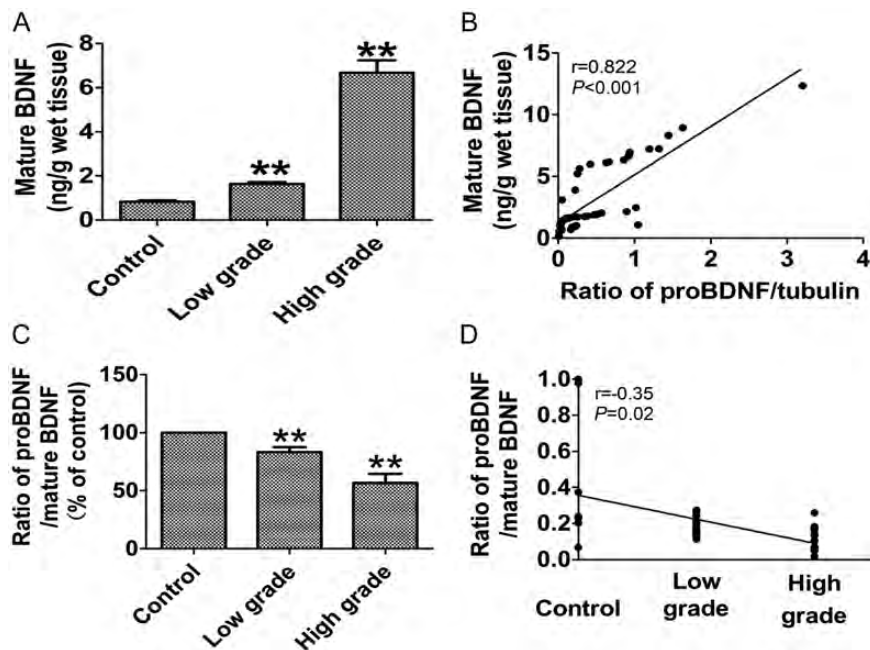


Fig. 5. Decreased ratio of proBDNF to mature BDNF in human high-grade glioma. (A) The levels of mature BDNF were assayed by ELISA. The concentration of mature BDNF was significantly increased 1.97-fold from normal to low grade (Mann–Whitney test,  $P < .001$ ) and 4.06-fold from low grade to high grade (Mann–Whitney test,  $P < .001$ ). (B) There was a positive correlation between proBDNF and mature BDNF levels (Spearman rank correlation,  $r = 0.822$ ,  $P < .001$ ). (C) The ratios of proBDNF to mature BDNF exhibited a significant decrease of 17% in low-grade gliomas (Mann–Whitney test,  $P = .002$ ) and 44% in high-grade gliomas compared with control (Mann–Whitney test,  $P < .001$ ), respectively. (D) The ratios of proBDNF to mature BDNF were negatively correlated with tumor grade (Spearman correlation,  $r = -0.35$ ,  $P = .02$ ).

proBDNF on C6 cell growth under serum-free conditions might be due to either increased cell death or decreased proliferation or both. Since p75NTR was expressed in C6 cells, we hypothesized that proBDNF might inhibit the growth of C6 cells through p75NTR. Indeed, the inhibitory effect of exogenous proBDNF (30 ng/mL) on C6 cell growth was abolished by p75NTR-ECD-Fc in the serum-free culture medium (Fig. 7C), suggesting that the inhibitory effect of proBDNF is dependent on p75NTR.

Since different concentrations of serum affected C6 cell growth in the presence of neurotrophins,<sup>44</sup> we tested whether serum concentration influenced C6 cell growth in the presence of different proBDNF doses. An MTT assay was performed in the presence of 5% FBS. In contrast to the absence of serum, the addition of proBDNF or anti-proBDNF had no significant impact on C6 glioma cell growth after a 48-h culture in the presence of 5% FBS (Supplementary Fig. S5A–C). To test whether proBDNF was degraded by proteases present in the serum, 50 ng proBDNF was incubated in culture medium in the presence or absence of 5% FBS in a CO<sub>2</sub> incubator overnight, and then a Western blot assay was performed. The membrane was incubated with sheep anti-proBDNF and sheep anti-mature BDNF simultaneously to see whether proBDNF was processed into mature BDNF. The result showed that proBDNF was decreased in 5% FBS culture medium and that no mature BDNF was detected (Supplementary Fig. S6).

#### ProBDNF Promoted Apoptosis of C6 Cells In vitro

To further evaluate the inhibitory effect of proBDNF on C6 glioma cells, we examined apoptosis of C6 glioma cells by DAPI nuclear staining. Treatment of anti-proBDNF significantly inhibited the apoptosis of C6 cells in a dose-dependent manner (Supplementary Fig. S7A, B, D). In contrast, C6 glioma cells treated with proBDNF (1, 3, 10, 30 ng/mL) in serum-free medium for 48 h significantly increased apoptosis in a dose-dependent manner. Treatment with 30 ng/mL recombinant proBDNF increased the number of dying cells by  $38.26 \pm 2.99\%$  compared with controls ( $P < .01$ ; Supplementary Fig. S7A, C, E). To study whether the effect of proBDNF on apoptosis was through p75NTR, 5  $\mu$ g/mL p75NTR-ECD-Fc was added in the culture medium supplemented with 30 ng/mL recombinant proBDNF. The result showed that the effect of proBDNF on C6 cell apoptosis was abolished by p75NTR-ECD-Fc (Supplementary Fig. S7E), suggesting that the effect of proBDNF is p75NTR dependent and that endogenous proBDNF may be able to induce the death of C6 glioma cells.

#### ProBDNF Reduced Motility and Invasion in C6 Glioma Cells

The increased GFAP expression of C6 cells by proBDNF may affect the motility and invasion of glioma cells. To test this hypothesis, we first examined the motility of C6

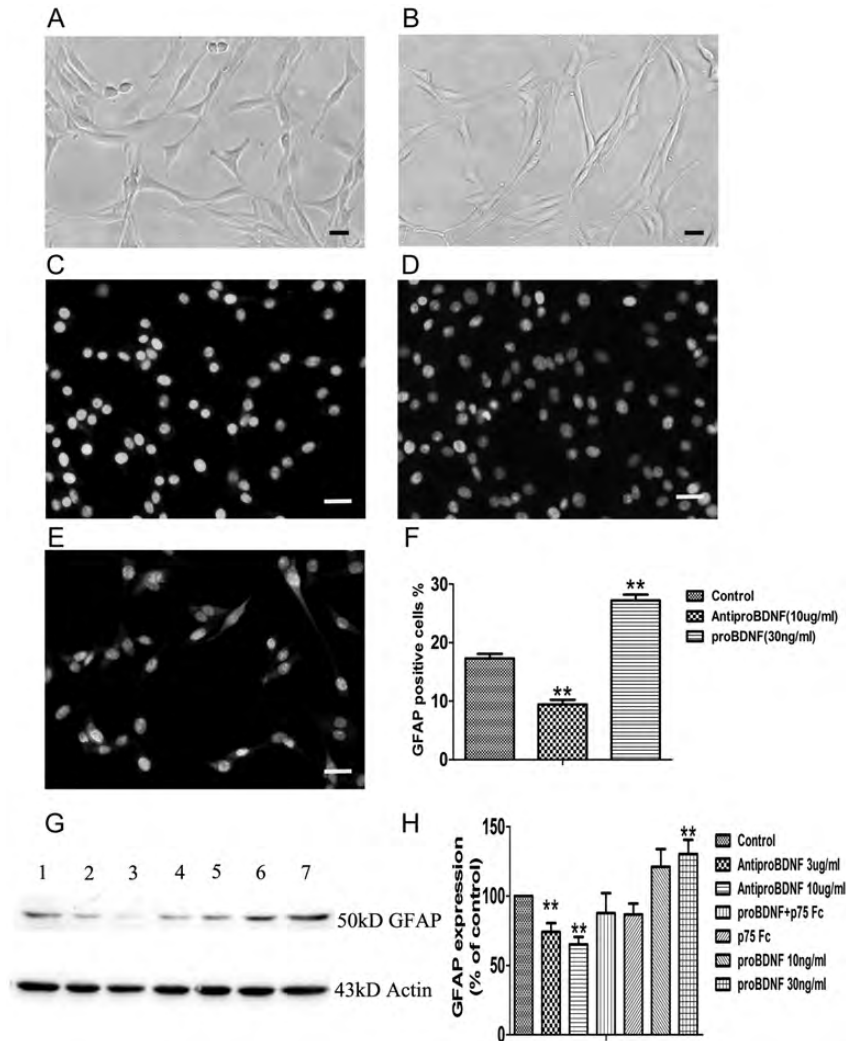


Fig. 6. Effect of recombinant proBDNF on C6 glioma cell morphological transformation and the expression of GFAP. (A) Control without treatment for 24 h. (B) Cells were treated with proBDNF (30 ng/mL) for 24 h. Treatment of proBDNF shows a remarkable change of morphology from polygonal shape to much longer, fine, tapering processes. (C–F) GFAP staining on C6 cells. (C) Untreated group. (D and F) Cell staining with Alexa 546 (red) showed that GFAP in C6 cells was significantly decreased after anti-proBDNF (10  $\mu$ g/mL) was added for 48 h, whereas (E and F) GFAP was increased after adding proBDNF (30 ng/mL) in the culture for 48 h compared with (C) untreated group. (G and H) Western blot analysis shows that GFAP in C6 cells is significantly decreased after adding anti-proBDNF (3–10  $\mu$ g/mL) for 48 h, whereas GFAP was increased after adding proBDNF (10–30 ng/mL) in the culture for 48 h compared with untreated group. P75NTR-ECD-Fc (5  $\mu$ g/mL) blocked the increased GFAP expression by proBDNF (lane 1: control, lane 2: anti-proBDNF 3  $\mu$ g/mL, lane 3: anti-proBDNF 10  $\mu$ g/mL, lane 4: p75NTR-ECD-Fc 5  $\mu$ g/mL, lane 5: proBDNF 30 ng/mL + p75NTR-ECD-Fc 5  $\mu$ g/mL, lane 6: proBDNF 10 ng/mL, lane 7: proBDNF 30 ng/mL). Data are presented as means  $\pm$  SE. Data points are the mean of triplicate assays. Scale bar, 25  $\mu$ m. \*\* $P < .01$ .

glioma cells in the presence of proBDNF and anti-proBDNF antibodies. By scratch assay, the proBDNF-treated C6 glioma cells exhibited decreased wound closure activity, while anti-proBDNF increased the activity (Supplementary Fig. S8). The effect of proBDNF on wound closure activity was blocked by the addition of p75NTR-ECD-Fc (Supplementary Fig. S8). Furthermore, we examined the effect of proBDNF on preventing the invasive nature of C6 glioma cells in a Boyden chamber assay. The results showed that the invasion of C6 glioma cells was inhibited significantly by the addition of proBDNF in a dose-dependent manner, whereas anti-

proBDNF increased the activity, and p75NTR-ECD-Fc abolished the effect of proBDNF (Fig. 8).

## Discussion

The aim of the present study was to elucidate the expression profile and functions of proBDNF and its receptors in glioma. Our results indicate that proBDNF and its receptors p75NTR and sortilin are highly expressed by glioma cells, particularly in high-grade glioma. We also found that proBDNF promotes apoptosis and differentiation

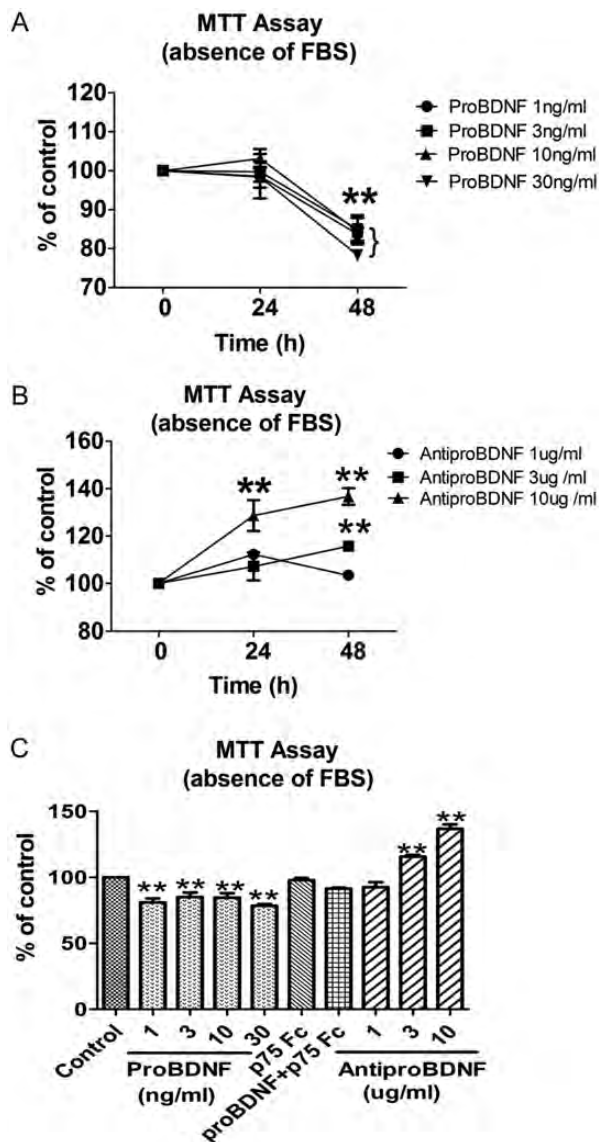


Fig. 7. Growth of C6 cells with proBDNF or anti-proBDNF treatment in serum-free medium. Cells were incubated in serum-free medium, supplemented with indicated concentrations of proBDNF (1, 3, 10, 30 ng/mL) or anti-proBDNF (1, 3, 10 µg/mL) in 96-well plates. MTT assays were performed after 0, 24, and 48 h for each treatment in triplicate. (A and C) ProBDNF inhibited C6 cell growth through p75NTR, whereas (B and C) anti-proBDNF promoted C6 cell survival under serum-free conditions after 48 h. Data are presented as means  $\pm$  SE. Results were replicated in at least 3 independent experiments. Controls were set as 100%. \*\* $P < .01$ .

of C6 glioma cells and suppresses their migration. Our data suggest that proBDNF may play an inhibitory role in glioma, in contrast to the roles of mature BDNF and its receptors.

#### Upregulation of ProBDNF and Its Receptors in Glioma

Previous studies have shown that *BDNF* mRNA is a prevalent transcript in the human frontal and temporal lobe

cortex,<sup>45</sup> which are the predilection sites of astrocytoma. Neurotrophin genes are widely expressed in 24 cell lines derived from human malignant gliomas, and the *BDNF* gene is most abundantly expressed.<sup>46</sup> In the present study, we have focused on the expression of proBDNF because it is a potent ligand of p75NTR,<sup>26</sup> which is highly expressed in glioma.<sup>18</sup> For the first time, our study systemically revealed the high expression of proBDNF and its receptor sortilin in human glioma. We found that *BDNF* mRNA and proBDNF are upregulated in advanced gliomas. Quantitative data show that the mRNA level in high-grade glioma is about 3-fold that of control tissues, and the proBDNF level is about 4-fold that of controls. The high expression of proBDNF in human gliomas is confirmed using Western blot, qRT-PCR, and immunostaining methods. In the present study, proBDNF, like mature BDNF, was predominantly detected in the cytoplasm of neurons in normal brain tissue, confirming previous findings.<sup>47,48</sup> The 34-kD peptide is the main form of proBDNF detected in normal human brain tissues and gliomas, but it is increased to a large degree in human high-grade gliomas compared with normal human brain tissues and low-grade gliomas. We found that proBDNF and fragments of 22 kD and 17 kD were all present. The 17-kD fragment is likely the prodomain generated from cleavage of the RR (diarginine) motif by furin. The existence of this fragment has been reported in neurons recently.<sup>49</sup> One important finding of the present study is that proBDNF immunoreactivity is obviously found in the nuclei of glioma cells. In normal control neurons or astrocytes, proBDNF is localized mainly in the cytoplasm. To verify the finding, we separated nuclear proteins from the cytoplasm of primary tumor cells. The function of proBDNF in the nuclei of tumor cells is not known, but the presence of proBDNF in the nuclei of tumor cells suggests that they may be involved in gene transcription. It would be worthwhile to further investigate whether the nuclear localization of proBDNF is related to the prognosis of the tumors.

The receptors of proBDNF—p75NTR and sortilin—are also upregulated in high-grade gliomas. This has been consistently supported by observations of IHC, Western blot, and qRT-PCR experiments. p75NTR is frequently expressed in advanced stages of human gliomas. High-grade glioma cells express significantly higher amounts of p75NTR compared with normal tissue and low-grade gliomas. The correlation data also indicate that p75NTR levels are positively correlated with tumor grades, suggesting that p75NTR may play a critical role in the pathogenesis of glioma. Our study is also consistent with previous studies in that p75NTR frequently exhibits robust expression in highly invasive glioblastoma specimens<sup>18</sup> and is a key regulator of glioma malignancy.<sup>18,41</sup>

The coreceptor of proBDNF, sortilin, is a member of the Vps10p-domain family of transmembrane receptors and mediates proneurotrophin-induced cell death.<sup>26,50</sup> Our data indicate that sortilin is highly upregulated in glioma. The levels of sortilin in high-grade tumors were 2- to 3-fold higher than in control tissues. The level of sortilin is positively correlated with tumor grade, indicating that sortilin may play a role in tumorigenesis. Sortilin is

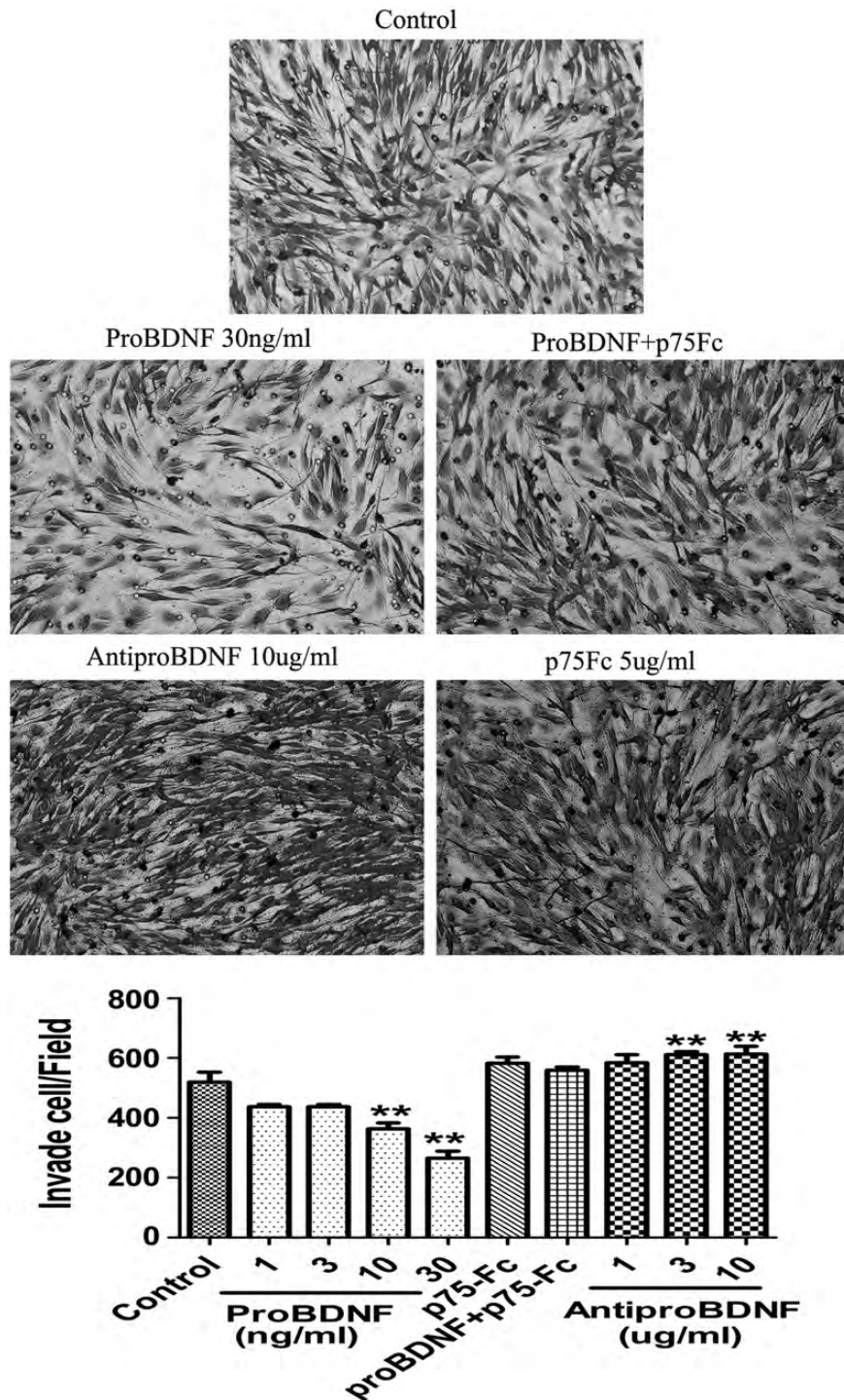


Fig. 8. Effect of proBDNF and anti-proBDNF on C6 cell invasion. Photomicrographs of C6 cells invaded through transwell membranes. Cells were treated with anti-proBDNF (10  $\mu$ g/mL), proBDNF (30 ng/mL), p75NTR-ECD-Fc (5  $\mu$ g/mL), or proBDNF (30 ng/mL) + p75NTR-ECD-Fc (5  $\mu$ g/mL) or were untreated for 24 h. The cells on the bottom of the insert were counted by DAPI staining and were stained with cresyl violet solution to confirm the DAPI stain data. Results were replicated in 3 independent experiments. Data were compared with control group. \*\* $P < .01$ .

localized mainly in the neuronal cytoplasm of controls and the cytoplasm of low-grade glioma cells. Our data show that sortilin is colocalized with proBDNF in the cytoplasm of control neurons, consistent with previous studies.<sup>26,51</sup> We also found that sortilin was localized in

some nuclei of glioma cells and that 95 kDa sortilin was present in the nuclear proteins from human glioma samples. Sortilin may play a role in proBDNF nuclear localization because the sortilin luminal domain interacts with proBDNF.<sup>26,51</sup>

### *ProBDNF Suppresses Tumor via Its Receptors*

The high expression of proBDNF and its receptors in high-grade glioma suggests that proBDNF may have an impact on the biology and progression of human glioma. Consistent with the results from tumor samples, the rat C6 glioma cell line also expresses proBDNF and its receptors. Furthermore, we found that proBDNF could be secreted into the medium, suggesting an autocrine or paracrine mechanism. Thus, C6 cells are a valid model to study the functions of proBDNF in glioma. Indeed, we found that proBDNF promoted the differentiation and apoptosis of C6 glioma cells and suppressed their growth and migration via p75NTR, suggesting that proBDNF and its receptors are likely to mediate an inhibitory signaling pathway on tumors.

ProBDNF may be able to promote the differentiation of C6 glioma cells. After proBDNF treatments, C6 glioma cells changed their shapes in culture. Most cells appeared as polygonal flattened shapes in normal culture medium but bore longer processes with narrow cell bodies after proBDNF treatment. GFAP is regarded as a marker of mature astrocytes, and its expression is often lost in malignant glioma grown in culture.<sup>41,43,52</sup> ProBDNF treatment significantly increases GFAP expression of C6 glioma cells, as shown by ICC and Western blots. Interestingly, the treatment of C6 glioma cells with anti-proBDNF to neutralize endogenous proBDNF decreased GFAP expression, which is consistent with the results of exogenous proBDNF. Our data also indicate that endogenous proBDNF secreted from C6 glioma cells promotes the differentiation of C6 cells. We found that the function of proBDNF in C6 glioma cell differentiation is p75NTR dependent, because p75NTR-ECD-Fc can reduce GFAP expression. These results strongly suggest that proBDNF promotes C6 glioma cell differentiation through p75NTR.

The differentiation of tumor cells is usually accompanied by cell cycle arrest.<sup>41,53</sup> Consistent with the data on differentiation, exogenous proBDNF induces a dose-dependent inhibition of C6 glioma cell growth and increases apoptosis. ProBDNF is likely to be potent in suppression of tumor cell growth, even effective at a concentration of 1 ng/mL. On the contrary, anti-proBDNF treatment increased cell growth but reduced apoptosis, indicating that endogenous proBDNF is functional in tumor suppression. Our result is consistent with a recent report showing that proBDNF suppresses the growth of the colorectal cancer cell.<sup>54</sup> Interestingly, the suppressive effect of proBDNF on C6 glioma cell growth is prevented by p75NTR-ECD-Fc.

It appears that the effect of proBDNF on cell growth is related to the serum levels in the culture medium. It is likely that growth factors present in the serum override the tumor-suppressive effect of proBDNF on tumor.<sup>44</sup> In addition, proBDNF may be degraded or cleaved to mature BDNF by proteolytic proteases in the serum, losing its tumor-suppressive effect. Indeed, we found that proBDNF is nonspecifically degraded in the presence of 5% serum (Supplementary Fig. S6). As we use the cleavage-resistant form of proBDNF (the cleavage site

RR of proBDNF is mutated into AA), no mature BDNF is observed under this condition.

The invasive property of a tumor often determines its malignancy and prognosis.<sup>55,56</sup> High-grade glioma is notorious for its invasiveness and rapid penetration to normal tissues.<sup>55,56</sup> A previous study has shown that p75NTR is a key molecule regulating infiltration of glioblastoma.<sup>18</sup> Our results indicate that proBDNF is effective in the suppression of cell infiltration and migration, as shown by 2 different assays, in a dose-dependent manner. The results from proBDNF neutralizing antibodies are consistent with those from exogenous proBDNF, promoting migration and invasion. Our data also indicate that the effect of proBDNF on cell migration is dependent on p75NTR, because using p75NTR-ECD-Fc attenuates its effect. Thus we propose that endogenous proBDNF secreted from glioma cells *in vivo* may suppress the invasion of glioma cells via its receptor p75NTR. However, our data are in high contrast to previous studies showing that p75NTR is a positive regulator of glioma migration and infiltration to normal brain tissues.<sup>18,57</sup> This difference in p75NTR function in the migration of glioma cells may depend on which ligands it binds. When p75NTR binds mature neurotrophins, as shown by Johnston et al,<sup>18</sup> p75NTR acts as an oncogenic factor-mediated invasion, and the activation of tumor cells results in striking cytoskeletal changes of the invading cells. In contrast, proBDNF, which forms the complex with the p75 receptor and sortilin,<sup>26</sup> may act as a tumor suppressor to inhibit cell migration and infiltration. Our previous studies on neurons have shown that proBDNF suppresses the migration of cerebellar granule cells and causes neurite collapse via p75NTR by activating RhoA.<sup>40</sup> It is well known that RhoA activation suppresses process growth and cell migration.<sup>33,58</sup> Thus our current study is consistent with the findings on functions of proBDNF in neurons that express both p75NTR and sortilin. Our result is also consistent with a recent report showing that p75NTR is a negative regulator of C6 glioma cell migration with neutralization antibodies to p75NTR.<sup>41</sup>

### *ProBDNF Versus Mature BDNF*

New evidence shows that proBDNF and mature BDNF elicit opposing effects via the p75NTR and tropomyosin-related kinase B (TrkB) receptors, respectively, in several physiological functions.<sup>26-30,32,33</sup> In our study the coexpression of proBDNF/p75NTR and proBDNF/sortilin is observed in human glioma samples by confocal microscopy. A recent study examined whether exogenous proBDNF significantly increased apoptotic ratios in primary colorectal cancer cell lines maintained in serum-free medium.<sup>54</sup> Considering the important roles of both proBDNF and mature BDNF in physiological functions, it would be informative to measure individual levels and the ratio of proBDNF and mature BDNF in human normal brain tissue and glioma samples.

BDNF and other neurotrophins are regarded as oncogenic factors in tumorigenesis, proliferation, and survival

in different types of tumors<sup>54,59,60</sup> and are correlated with poor prognosis in various TrkB-expressing human cancers, including tumors in the nervous system.<sup>61,62</sup> In our study, both proBDNF and mature BDNF were significantly increased in high-grade glioma tissues, but mature BDNF showed a much greater increase. The ratio of proBDNF to mature BDNF levels is decreased in high-grade glioma tissues and is negatively correlated with tumor grade. Therefore, it is likely that increased levels of mature BDNF contribute mainly to tumorigenesis, as observed in earlier reports.<sup>54,59,60</sup> ProBDNF may have an opposite function to its mature form in tumorigenesis through p75NTR and sortilin, as known in neurons.<sup>26–28,32</sup> These findings suggest that the proBDNF-p75-sortilin pathway may be a balancing signal to tumor growth by the mature BDNF-TrkB pathway and other tumor growth signals, such as epidermal growth factor,<sup>63,64</sup> platelet derived growth factor,<sup>65–67</sup> and neuregulin.<sup>68,69</sup> The opposing role played by proBDNF may be critical to prevent high-grade tumors from overaggression. The relative expression levels of proBDNF and mature BDNF may determine the balance of these 2 signaling pathways in the malignancy and prognosis of glioma. Given the opposing functions of proBDNF and mature BDNF in glioma, it would be of great interest to study the precise mechanisms controlling the relative expression levels of proBDNF and mature BDNF in the malignancy and prognosis of glioma.

High-grade gliomas are associated with heterogeneity of clinical manifestation, image characteristics, and histopathological findings.<sup>70</sup> Malignant gliomas are characterized by their invasiveness and angiogenesis<sup>71</sup> and are necrosis prone.<sup>34</sup> The microenvironment change in malignant glioma will lead to the change of a series of growth factor signals.<sup>72,73</sup> An imbalance between levels of proBDNF and mature BDNF in a “tumor microenvironment” might contribute to tumor cell growth and invasion. Proteases play a decisive role in this malignant process, either by degradation of brain extracellular matrix components and adhesion molecules or by regulating the activity of growth and chemotactic factors.<sup>74,75</sup> ProBDNF-converting enzymes such as MMPs or tissue plasminogen activator (tPA) are produced and released by glioma cells.<sup>75–79</sup> The constitutive overexpression of

MMPs is frequently observed in malignant tumors. In particular, MMP-2 and MMP-9 have been reported to be closely associated with invasion and angiogenesis in malignant gliomas.<sup>80</sup> A relative reduction in tPA in glioma tissue may play an integral role in the development of tissue necrosis and tissue edema.<sup>81,82</sup> Expression of tPA is detected during the entire glioma growth, while later in the time course the expression is found predominantly in the invasive border of the tumor.<sup>83</sup> Thus, modification of the proBDNF signaling pathway by supplement of cleavage-resistant proBDNF or the inhibition of proBDNF-converting enzymes such as furin, tPA, or MMPs<sup>25,84,85</sup> might have a therapeutic significance in this tumor.

## Conclusion

Taken together, our data illustrate that proBDNF and its receptors p75NTR and sortilin are highly upregulated in high-grade glioma in humans. Using C6 cells as a model, we have also demonstrated that proBDNF is a potent tumor suppressor by promoting differentiation and death and by inhibiting the growth and migration of C6 cells via p75NTR in vitro. Our study suggests that the modification of the proBDNF signaling pathway may be useful to suppress the growth of high-grade gliomas.

## Supplementary Material

Supplementary material is available online at *Neuro-Oncology* (<http://neuro-oncology.oxfordjournals.org/>).

## Funding

This work was supported by grants from Chinese MST 2011CB944200, a Talent grant of Yunnan Province Government (to Z-C.X.) and Australian National Health and Medical Research Council (595937). X-F.Z. is a visiting professor of Kunming Medical University.

*Conflict of interest statement.* None declared.

## References

1. Kesari S, Stiles CD. The bad seed: PDGF receptors link adult neural progenitors to glioma stem cells. *Neuron*. 2006;51:151–153.
2. Boring CC, Squires TS, Tong T, Montgomery S. Cancer statistics, 1994. CA: *Cancer J Clin*. 1994;44:7–26.
3. Brada M, Sharpe G, Rajan B, et al. Modifying radical radiotherapy in high grade gliomas; shortening the treatment time through acceleration. *Int J Rad Oncol Biol Phys*. 1999;43:287–292.
4. Winger MJ, Macdonald DR, Cairncross JG. Supratentorial anaplastic gliomas in adults. The prognostic importance of extent of resection and prior low-grade glioma. *J Neurosurg*. 1989;71:487–493.
5. Shibamoto Y, Yamashita J, Takahashi M, Yamasaki T, Kikuchi H, Abe M. Supratentorial malignant glioma: an analysis of radiation therapy in 178 cases. *Radiother Oncol*. 1990;18:9–17.
6. Reni M, Cozzarini C, Ferreri AJ, et al. A retrospective analysis of postirradiation chemotherapy in 133 patients with glioblastoma multiforme. *Cancer Invest*. 2000;18:510–515.
7. Brada M, Baumert B. Focal fractionated conformal stereotactic boost following conventional radiotherapy of high-grade gliomas: a randomized phase III study. A joint study of the EORTC (22972) and the MRC (BR10). *Front Rad Ther Oncol*. 1999;33:241–243.
8. Bleehen NM, Stenning SP. A Medical Research Council trial of two radiotherapy doses in the treatment of grades 3 and 4 astrocytoma. The Medical Research Council Brain Tumour Working Party. *Br J Cancer*. 1991;64:769–774.
9. Holland EC. Gliomagenesis: genetic alterations and mouse models. *Nat Rev Genet*. 2001;2:120–129.



10. Frei K. Genes and pathways driving glioblastomas in humans and murine disease models. *Neurosurg Rev.* 2003;26:161.
11. Bachoo RM, Maher EA, Ligon KL, et al. Epidermal growth factor receptor and Ink4a/Arf: convergent mechanisms governing terminal differentiation and transformation along the neural stem cell to astrocyte axis. *Cancer Cell.* 2002;1:269–277.
12. Uhrbom L, Dai C, Celestino JC, Rosenblum MK, Fuller GN, Holland EC. Ink4a-Arf loss cooperates with KRas activation in astrocytes and neural progenitors to generate glioblastomas of various morphologies depending on activated Akt. *Cancer Res.* 2002;62:5551–5558.
13. Bajenaru ML, Hernandez MR, Perry A, et al. Optic nerve glioma in mice requires astrocyte Nf1 gene inactivation and Nf1 brain heterozygosity. *Cancer Res.* 2003;63:8573–8577.
14. Kwon CH, Zhao D, Chen J, et al. PTEN haploinsufficiency accelerates formation of high-grade astrocytomas. *Cancer Res.* 2008;68:3286–3294.
15. Merlo A. Genes and pathways driving glioblastomas in humans and murine disease models. *Neurosurg Rev.* 2003;26:145–158.
16. de la Iglesia N, Puram SV, Bonni A. STAT3 regulation of glioblastoma pathogenesis. *Curr Mol Med.* 2009;9:580–590.
17. Bernstein JJ, Woodard CA. Glioblastoma cells do not intravasate into blood vessels. *Neurosurgery.* 1995;36:124–132, discussion 132.
18. Johnston AL, Lun X, Rahn JJ, et al. The p75 neurotrophin receptor is a central regulator of glioma invasion. *PLoS Biol.* 2007;5:e212.
19. Juric DM, Miklic S, Carman-Krzan M. Monoaminergic neuronal activity up-regulates BDNF synthesis in cultured neonatal rat astrocytes. *Brain Res.* 2006;1108:54–62.
20. Elmariah SB, Hughes EG, Oh EJ, Balice-Gordon RJ. Neurotrophin signaling among neurons and glia during formation of tripartite synapses. *Neuron Glia Biol.* 2005;1:1–11.
21. Miklic S, Juric DM, Carman-Krzan M. Differences in the regulation of BDNF and NGF synthesis in cultured neonatal rat astrocytes. *Int J Dev Neurosci.* 2004;22:119–130.
22. Seidah NG, Chretien M. Proprotein and prohormone convertases: a family of subtilases generating diverse bioactive polypeptides. *Brain Res.* 1999;848:45–62.
23. Barker PA. Whither proBDNF? *Nat Neurosci.* 2009;12:105–106.
24. Zhou XF, Song XY, Zhong JH, Barati S, Zhou FH, Johnson SM. Distribution and localization of pro-brain-derived neurotrophic factor-like immunoreactivity in the peripheral and central nervous system of the adult rat. *J Neurochem.* 2004;91:704–715.
25. Pang PT, Teng HK, Zaitsev E, et al. Cleavage of proBDNF by tPA/plasmin is essential for long-term hippocampal plasticity. *Science.* 2004;306:487–491.
26. Teng HK, Teng KK, Lee R, et al. ProBDNF induces neuronal apoptosis via activation of a receptor complex of p75NTR and sortilin. *J Neurosci.* 2005;25:5455–5463.
27. Kenchappa RS, Zampieri N, Chao MV, et al. Ligand-dependent cleavage of the P75 neurotrophin receptor is necessary for NRIF nuclear translocation and apoptosis in sympathetic neurons. *Neuron.* 2006;50:219–232.
28. Fan YJ, Wu LL, Li HY, Wang YJ, Zhou XF. Differential effects of pro-BDNF on sensory neurons after sciatic nerve transection in neonatal rats. *Eur J Neurosci.* 2008;27:2380–2390.
29. Woo NH, Teng HK, Siao CJ, et al. Activation of p75NTR by proBDNF facilitates hippocampal long-term depression. *Nat Neurosci.* 2005;8:1069–1077.
30. Lu B. Pro-region of neurotrophins: role in synaptic modulation. *Neuron.* 2003;39:735–738.
31. Lu B, Pang PT, Woo NH. The yin and yang of neurotrophin action. *Nat Rev Neurosci.* 2005;6:603–614.
32. Koshimizu H, Hazama S, Hara T, Ogura A, Kojima M. Distinct signaling pathways of precursor BDNF and mature BDNF in cultured cerebellar granule neurons. *Neurosci Lett.* 2010;473:229–232.
33. Sun Y, Lim Y, Li F, et al. ProBDNF collapses neurite outgrowth of primary neurons by activating RhoA. *PLoS One.* 2012;7:e35883.
34. Louis DN, Ohgaki H, Wiestler OD, et al. The 2007 WHO classification of tumours of the central nervous system. *Acta Neuropathologica.* 2007;114:97–109.
35. Gimenez M, Souza VC, Izumi C, et al. Proteomic analysis of low- to high-grade astrocytomas reveals an alteration of the expression level of raf kinase inhibitor protein and nucleophosmin. *Proteomics.* 2010;10:2812–2821.
36. Moss SF, Lee JW, Sabo E, et al. Decreased expression of gastrokine 1 and the trefoil factor interacting protein TFIZ1/GKN2 in gastric cancer: influence of tumor histology and relationship to prognosis. *Clin Cancer Res.* 2008;14:4161–4167.
37. Livak KJ, Schmittgen TD. Analysis of relative gene expression data using real-time quantitative PCR and the 2(-delta delta C(T)) method. *Methods.* 2001;25:402–408.
38. Keifer J, Sabirzhanov BE, Zheng Z, Li W, Clark TG. Cleavage of proBDNF to BDNF by a tolloid-like metalloproteinase is required for acquisition of in vitro eyeblink classical conditioning. *J Neurosci.* 2009;29:14956–14964.
39. Kelly KJ, Sandoval RM, Dunn KW, Molitoris BA, Dagher PC. A novel method to determine specificity and sensitivity of the TUNEL reaction in the quantitation of apoptosis. *Am J Cell Physiol.* 2003;284:C1309–C1318.
40. Xu ZQ, Sun Y, Li HY, Lim Y, Zhong JH, Zhou XF. Endogenous proBDNF is a negative regulator of migration of cerebellar granule cells in neonatal mice. *Eur J Neurosci.* 2011;33:1376–1384.
41. Lin WL, Liang WH, Lee YJ, Chuang SK, Tseng TH. Antitumor progression potential of caffeic acid phenethyl ester involving p75(NTR) in C6 glioma cells. *Chem-Biol Interact.* 2010;188:607–615.
42. Raju TR, Bignami A, Dahl D. Glial fibrillary acidic protein in monolayer cultures of C-6 glioma cells: effect of aging and dibutyl cyclic AMP. *Brain Res.* 1980;200:225–230.
43. Tabuchi K, Furuta T, Norikane H, Tsuboi M, Moriya Y, Nishimoto A. Evaluation of the drug-induced morphological differentiation of rat glioma cells (C-6) from the aspects of S-100 protein level and con A binding pattern. *J Neurol Sci.* 1981;51:119–130.
44. Weis C, Wiesenhofer B, Humpel C. Nerve growth factor plays a divergent role in mediating growth of rat C6 glioma cells via binding to the p75 neurotrophin receptor. *J Neuro-Oncol.* 2002;56:59–67.
45. Lichter T, Yamamoto H, Gurney ME. Gene expression of neurotrophic factors in human brain tumors. *Mol Cell Neurosci.* 1991;2:168–171.
46. Hamel W, Westphal M, Szonyi E, Escandon E, Nikolics K. Neurotrophin gene expression by cell lines derived from human gliomas. *J Neurosci Res.* 1993;34:147–157.
47. Fahnestock M, Garzon D, Holsinger RM, Michalski B. Neurotrophic factors and Alzheimer's disease: are we focusing on the wrong molecule? *J Neural Trans Suppl.* 2002;62:241–252.
48. Peng S, Wu J, Mufson EJ, Fahnestock M. Precursor form of brain-derived neurotrophic factor and mature brain-derived neurotrophic factor are decreased in the pre-clinical stages of Alzheimer's disease. *J Neurochem.* 2005;93:1412–1421.
49. Dieni S, Matsumoto T, Dekkers M, et al. BDNF and its pro-peptide are stored in presynaptic dense core vesicles in brain neurons. *J Cell Biol.* 2012;196:775–788.
50. Nykjaer A, Lee R, Teng KK, et al. Sortilin is essential for proNGF-induced neuronal cell death. *Nature.* 2004;427:843–848.

51. Yang M, Lim Y, Li X, Zhong JH, Zhou XF. Precursor of brain-derived neurotrophic factor (proBDNF) forms a complex with Huntingtin-associated protein-1 (HAP1) and sortilin that modulates proBDNF trafficking, degradation, and processing. *J Biol Chem*. 2011;286:16272–16284.
52. Yusubaliev GM, Baklaushev VP, Gurina OI, Tsitrin EB, Chekhonin VP. Immunohistochemical analysis of glial fibrillary acidic protein as a tool to assess astroglial reaction in experimental C6 glioma. *Bull Exper Biol Med*. 2010;149:125–130.
53. He S, Zhu W, Zhou Y, et al. Transcriptional and post-transcriptional down-regulation of cyclin D1 contributes to C6 glioma cell differentiation induced by forskolin. *J Cell Biochem*. 2011;112:2241–2249.
54. Akil H, Perraud A, Melin C, Jauberteau MO, Mathonnet M. Fine-tuning roles of endogenous brain-derived neurotrophic factor. TrkB and sortilin in colorectal cancer cell survival. *PLoS One*. 2011;6:e25097.
55. Winkler F, Kienast Y, Fuhrmann M, et al. Imaging glioma cell invasion in vivo reveals mechanisms of dissemination and peritumoral angiogenesis. *Glia*. 2009;57:1306–1315.
56. Goebell E, Paustenbach S, Vaeterlein O, et al. Low-grade and anaplastic gliomas: differences in architecture evaluated with diffusion-tensor MR imaging. *Radiology*. 2006;239:217–222.
57. Wang L, Rahn JJ, Lun X, et al. Gamma-secretase represents a therapeutic target for the treatment of invasive glioma mediated by the p75 neurotrophin receptor. *PLoS Biol*. 2008;6:e289.
58. Gehler S, Gallo G, Veien E, Letourneau PC. p75 neurotrophin receptor signaling regulates growth cone filopodial dynamics through modulating RhoA activity. *J Neurosci*. 2004;24:4363–4372.
59. Hu Y, Wang YD, Guo T, et al. Identification of brain-derived neurotrophic factor as a novel angiogenic protein in multiple myeloma. *Cancer Genet Cytogenet*. 2007;178:1–10.
60. Fauchais AL, Lalloue F, Lise MC, et al. Role of endogenous brain-derived neurotrophic factor and sortilin in B cell survival. *J Immunol*. 2008;181:3027–3038.
61. Nakagawara A, Azar CG, Scavarda NJ, Brodeur GM. Expression and function of TRK-B and BDNF in human neuroblastomas. *Mol Cell Biol*. 1994;14:759–767.
62. Stephan H, Zakrzewski JL, Boloni R, Grasmann C, Lohmann DR, Eggert A. Neurotrophin receptor expression in human primary retinoblastomas and retinoblastoma cell lines. *Pediatr Blood Cancer*. 2008;50:218–222.
63. Pickhard AC, Margraf J, Knopf A, et al. Inhibition of radiation induced migration of human head and neck squamous cell carcinoma cells by blocking of EGF receptor pathways. *BMC Cancer*. 2011;11:388.
64. Ji H, Wang J, Nika H, et al. EGF-induced ERK activation promotes CK2-mediated disassociation of alpha-catenin from beta-catenin and transactivation of beta-catenin. *Mol Cell*. 2009;36:547–559.
65. Nazarenko I, Hede SM, He X, et al. PDGF and PDGF receptors in glioma. *Uppsala J Med Sci*. 2012;117:99–112.
66. Lokker NA, Sullivan CM, Hollenbach SJ, Israel MA, Giese NA. Platelet-derived growth factor (PDGF) autocrine signaling regulates survival and mitogenic pathways in glioblastoma cells: evidence that the novel PDGF-C and PDGF-D ligands may play a role in the development of brain tumors. *Cancer Res*. 2002;62:3729–3735.
67. Ranza E, Facchetti A, Morbini P, Benericetti E, Nano R. Exogenous platelet-derived growth factor (PDGF) induces human astrocytoma cell line proliferation. *Anticancer Res*. 2007;27:2161–2166.
68. Ritch PS, Carroll SL, Sontheimer H. Neuregulin-1 enhances survival of human astrocytic glioma cells. *Glia*. 2005;51:217–228.
69. Ritch PA, Carroll SL, Sontheimer H. Neuregulin-1 enhances motility and migration of human astrocytic glioma cells. *J Biol Chem*. 2003;278:20971–20978.
70. Okajima K, Ohta Y. [Diagnostic imaging of high-grade astrocytoma: heterogeneity of clinical manifestation, image characteristics, and histopathological findings]. *Shinkei Kenkyu No Shinpo [Brain Nerve]*. 2012;64:1151–1157.
71. Brell M, Ibanez J, Felpete A, Burguera B, Frontera M, Couce ME. Quantitative analysis of matrix metalloproteinase-2 mRNA expression in central and peripheral regions of gliomas. *Brain Tumor Pathol*. 2011;28:137–144.
72. Kruttgen A, Schneider I, Weis J. The dark side of the NGF family: neurotrophins in neoplasias. *Brain Pathol*. 2006;16:304–310.
73. Hanahan D, Weinberg RA. Hallmarks of cancer: the next generation. *Cell*. 2011;144:646–674.
74. Mentlein R, Hattermann K, Held-Feindt J. Lost in disruption: role of proteases in glioma invasion and progression. *Biochim Biophys Acta*. 2012;1825:178–185.
75. Levicar N, Nuttall RK, Lah TT. Proteases in brain tumour progression. *Acta Neurochir*. 2003;145:825–838.
76. Salmaggi A, Croci D, Prina P, et al. Production and post-surgical modification of VEGF, tPA and PAI-1 in patients with glioma. *Cancer Biol Ther*. 2006;5:204–209.
77. Akai T, Niiya K, Sakuragawa N, Iizuka H, Endo S. Modulation of tissue-type plasminogen activator expression by platelet activating factor in human glioma cells. *J Neuro-Oncol*. 2002;59:193–198.
78. Hagemann C, Anacker J, Ernestus RI, Vince GH. A complete compilation of matrix metalloproteinase expression in human malignant gliomas. *World J Clin Oncol*. 2012;3:67–79.
79. Takano S, Mashiko R, Osuka S, Ishikawa E, Ohneda O, Matsumura A. Detection of failure of bevacizumab treatment for malignant glioma based on urinary matrix metalloproteinase activity. *Brain Tumor Pathol*. 2010;27:89–94.
80. Nakabayashi H, Yawata T, Shimizu K. Anti-invasive and antiangiogenic effects of MMI-166 on malignant glioma cells. *BMC Cancer*. 2010;10:339.
81. Sawaya R, Ramo OJ, Shi ML, Mandybur G. Biological significance of tissue plasminogen activator content in brain tumors. *J Neurosurg*. 1991;74:480–486.
82. Bindal AK, Hammoud M, Shi WM, Wu SZ, Sawaya R, Rao JS. Prognostic significance of proteolytic enzymes in human brain tumors. *J Neuro-Oncol*. 1994;22:101–110.
83. Sandstrom M, Johansson M, Sandstrom J, Bergenheim AT, Henriksson R. Expression of the proteolytic factors, tPA and uPA, PAI-1 and VEGF during malignant glioma progression. *Int J Dev Neurosci*. 1999;17:473–481.
84. Marcinkiewicz M, Seidah NG, Chretien M. Implications of the subtilisin/kexin-like precursor convertases in the development and function of nervous tissues. *Acta Neurobiol Exper*. 1996;56:287–298.
85. Yoshida T, Ishikawa M, Niitsu T, et al. Decreased serum levels of mature brain-derived neurotrophic factor (BDNF), but not its precursor proBDNF, in patients with major depressive disorder. *PLoS One*. 2012;7:e42676.